Journal of Applied Fluid Mechanics , Vol. 8, No. 3, pp. 339-350, 2015.
Available online at www.jafmonline.net, ISSN 1735-3572, EISSN 1735-3645.
DOI: 10.18869/acadpub.jafm.67.222.23135

Stokes Flow over Composite Sphere: Liquid Core with Permeable Shell

B.R. Jaiswal[1†] and B.R.Gupta[2]

[1] *Department of Mathematics, Jaypee University of Engineering & Technology, Guna, M.P., 473226, India*
[2] *Department of Mathematics, Jaypee University of Engineering & Technology, Guna, M.P., 473226, India*

† *Corresponding Author Email*: *jaiswal.bharat@gmail.com*

(Received May 19 2014; accepted June 19 2014)

ABSTRACT

This paper presents an analytical study of an infinite expanse of uniform flow of steady axisymmetric Stokes flow of an incompressible Newtonian fluid around the spherical drop of Reiner-Rivlin liquid coated with the permeable layer with the assumption that the liquid located outside the capsule penetrates into the permeable layer, but it is not mingled with the liquid located in the internal concave of capsule. The flow inside the permeable layer is described by the Brinkman equation. The viscosity of the permeable medium is assumed to be same as pure liquid. The stream function solution for the outer flow field is obtained in terms of modified Bessel functions and Gegenbauer functions, and for the inner flow field, the stream function solution is obtained by expanding the stream function in terms of S. The flow fields are determined explicitly by matching the boundary conditions at the pure liquid-porous interface, porous-Reiner-Rivlin liquid interface, and uniform velocity at infinity. The drag force experienced by the capsule is evaluated, and its variation with regard to permeability parameter α, dimensionless parameter S, ratio of viscosities λ^2, and thickness of permeable layer δ is studied and graphs plotted against these parameters. Several cases of interest are deduced from the present analysis. It is observed that the cross-viscosity increases the drag force, whereas the thickness δ decreases the drag on capsule. It is also observed that the drag force is increasing or decreasing function of permeability parameter for $\lambda^2 < 1$.

Keywords: Brinkman equation; Drag force; Modified Bessel functions; Reiner-Rivlin liquid; Permeability parameter; Stream functions; Permeable spherical shell.

NOMENCLATURE

a	radius of the liquid sphere
b	radius of the outer permeable shell
D_N	dimensionless drag
F	drag force
$P_n(\zeta)$	Legendre functions
S	dimensionless parameter
r, θ, ϕ	spherical polar coordinates
$\mathbf{u}^{(i)}$	velocity vectors
μ_c	cross viscosity
$y_n(\alpha r), y_{-n}(\alpha r)$	modified Bessel functions
μ_1, μ_3	viscosity coefficients
μ_e	effective viscosity of permeable region
κ	permeability
$\psi^{(i)}(r, \zeta)$	stream functions
$\tau_{rr}, \tau_{r\theta}$	dimensionless stress components
λ^2	relative viscosity(μ_1/μ_3)
δ	thickness of permeable layer
α	permeability parameter

1. INTRODUCTION

The study of viscous flow through permeable media has attracted substantial practical and theoretical interest in science, engineering, and technology. The flow through permeable media takes place generally in geophysical and bio-mechanical problems and also has many engineering applications, such as, flow in fixed beds, petroleum industry, hydrology, lubrication problems, etc. The most practical example of physical process of viscous flow within a permeable spherical region is the structure of the earth. Due to its broad areas of applications in science, engineering and industries, many different theoretical and experimental models have been used for describing the viscous flow past and through the solids or porous bodies. For efficient and effective utilization of bodies

with porous structured in the above mentioned areas, the structure of porous lamina must be considered and analyzed from all point of views. For analytical study of the fluid flows within porous structured bodies, so called porous media, the two terms: porosity and permeability, play significant and vital role. The porosity is the measure of how much of a porous material has tiny spaces in it. More precisely, it is defined as the ratio of voids' volume to that of the volume of the material. Theoretically, it seems that if the material has more pores (voids), it will allow the fluid to pass through it easily, but actually it is not so and could be understood through the permeability which is defined as the easiness or ability (inter connectivity of pores) of the material to allow the fluids to pass through it. The first model that was initially introduced to analyze the fluid flow in permeable media was Darcy's law by Darcy (1856). In his proposed model he stated that the rate of flow in porous media (through a densely packed bed of fine particles) is proportional to pressure gradient. This model was broadly used as the basic model in literature. Several studies of the flow field within and outside porous spheres are limited mainly to low Reynolds numbers. Joseph and Tao (1964) investigated the problem of creeping flow past a porous spherical shell immersed in a uniform steady, viscous, and incompressible fluid using Darcy's law for the flow inside the porous region and Stokes equations for the fluid outside the sphere using no-slip condition for tangential velocity component at the surface of the sphere and reported that the drag on the porous sphere is the same as that of a rigid sphere with minimized radius. Padmavathi *et al.* (1994) have solved the problem of creeping flow past a porous sphere immersed in a uniform viscous incompressible fluid using Darcy's law taking into account the Saffman boundary condition in place of no-slip boundary condition at the surface of the sphere. Whereas, Sutherland and Tan (1970) assumed continuity of the tangential velocity component at the sphere surface. However, Darcy's law seems to be inadequate for the flows with high porosity. Most of the early authors like Boutros *et al.* (2006), Mukhopadhyay and Layek (2009) etc. applied various types of extended Darcy models on convection in porous media. During nineteenth century, after the Darcy's work, flow through porous media was influenced and emulated by questions emerging in practical problems. To study the flows with high porosity media and large shear rates, Brinkman (1947) proposed a modification to Darcy's law which was assumed to be governed by a swarm of homogeneous spherical particles by appending a Laplacian term in velocity and is commonly known as Brinkman's equation. Experimental results of Ooms *et al.* (1970), and Matsumoto and Suganuma (1977) are theoretically verified by Tam (1969), and Lundgren (1972) established the validity of the Brinkman's equation. The problem of creeping flow relative to permeable spheres was solved by Neale *et al.* (1973). Higdon and Kojima (1981) have studied the Stokes flow past porous particles using the Brinkman's equation for the flow inside the porous media and derived some asymptotic results in case of low and high permeability by using Greens function formulation of the Brinkman's equation. A numerical study was done by Nandkumar and Masliyah (1982) to investigate the flow field within and around an isolated porous sphere taking into account the low Reynolds number using the Brinkman's equation for the internal flow field. The computed hydrodynamic resistances were found to agree with the experiments on settling of porous spheres by Masliyah and Polikar (1980). By using Stokes approximation, Birikh and Rudakoh (1982) investigated the problem of slow motion of a permeable sphere in a viscous fluid and calculated the drag and the flow rate of the fluid. Masliyah *et al.* (1987) solved analytically the problem of creeping flow past a sphere having solid core with porous shell and found that the results are in excellent agreement with the experimental ones. Using this Brinkman's equation for the flow inside the permeable sphere, Qin and Kaloni (1988) obtained a Cartesian-tensor solution for the flow of incompressible viscous fluid past a porous sphere and evaluated the hydro dynamical force experienced by a porous sphere and also discussed and laid emphasis on the merits of Brinkman's equation over Darcy's equation. Bhatt and Sacheti (1994) have studied the problem of viscous flow past a porous spherical shell using the Brinkman's model and they evaluated the drag force experienced by the shell. Barman (1996) has investigated the problem of a Newtonian fluid past an impervious sphere embedded in a constant permeable medium by applying Brinkman's model and he obtained an exact solution to the governing equations in terms of stream function setting forth constant velocity far from the sphere. Using the stream function formulation, Zlatanovski (1999) obtained a convergent series solution to the Brinkman's equation for the problem of creeping flow past a porous prolate spheroidal particle and recovered the solution for flow past a porous spherical particle as a limiting case of the spheroidal particle. Srinivasacharya (2003) has discussed the creeping flow of a viscous fluid past and through a porous approximate sphere neglecting inertia terms, and deduced the result for an oblate spheroid in an unbounded medium. The motion of a porous sphere in a spherical container using Brinkman's model in the porous region was studied by Srinivasacharya (2005). Deo and Gupta (2009) investigated the problem of sym-

metrical creeping flow of an incompressible viscous fluid past a swarm of porous approximately spheroidal particles with Kuwabara boundary condition with vanishing vorticity on the boundary. Recently, Deo and Gupta (2010) have evaluated the drag force on a porous sphere embedded in another porous medium. Yadav *et al.* (2010) have evaluated the hydrodynamic permeability of membranes built up by spherical particles covered by porous shells. The problem of the flow around particles with porous shell, and the filtration of viscous liquid in the porous medium with complex internal structure are closely interconnected.

At present, authors are paying much attention on keen and thorough study of microcapsules. As these microcapsules are used for supplying of drugs and reagents. Modern microcapsules represent porous shells that may contain either desired particles or liquids. The properties of porous media differ from the properties of a dispersion medium. These capsules are of very great importance for modern nanotechnologies and are characterized by diverse values of their parameters. Hence, the theoretical prediction of the hydrodynamic behavior of microcapsules presents not only mathematical interest, but can also be useful for the formation and application of encapsulated media. The motion of capsules in the flow of liquid is of great applied and theoretical interest. There are developments that involve the encapsulation of anticorrosive additives for paint and lacquer coatings. In all of these cases, the motion of the drop-shell system relative to the external flow occurs either at the material production stage or in the practical use of capsules. Sekhar and Bhattacharyya (2005) used stress jump boundary condition to study the Stokes flow of a viscous fluid inside a sphere with internal singularities enclosed by a porous spherical shell, and concluded that the fluid velocity at a porous-liquid interface varies with the stress jump coefficient and plays an important role in describing the flow field associated with porous medium. Vasin and Kharitonova (2011a) investigated the problem of a viscous liquid flow past a spherical porous capsule. Stokes flow of an assemblage of porous particles was studied by Prakash *et al.* (2011). Vasin and Kharitonova (2011b) solved the problem of the flow around the encapsulated drop of Newtonian liquid. In these right above discussed problems, authors have taken into consideration the tangential stress jump condition on the porous - pure liquid interface. Ramkissoon and Rahaman (2001) solved the problem of Non-Newtonian fluid sphere in a spherical container and found that cross-viscosity decreases the wall effects. Recently, Jaiswal and Gupta (2014a) solved a problem of Reiner-Rivlin liquid sphere placed in micro-polar fluid with non-zero boundary condition for micro-rotation and found that spin parameter τ decreases the drag on the body. And later, the same problem was re-investigated by Jaiswal and Gupta (2014b), Jaiswal and Gupta (2015), respectively, for the case of non-Newtonian liquid spheroid in spherical container, and non-Newtonian liquid sphere embedded in a porous medium saturated with Newtonian fluid. All these investigations mentioned above, motivated us to study the slow viscous flow past and within a spherical shell encapsulated by non-Newtonian liquid.

In this paper, we consider the problem of steady axisymmetric creeping flow of Newtonian fluid around the capsule that contains the non-Newtonian liquid which can not flow out of the permeable layer, but the liquid outside the capsule can permeates into the porous layer. Both, the internal and external, flow fields are determined by using the stokes approximation and expanding the internal stream function in powers of a dimensionless parameter S. The flow within the permeable region of the capsule is governed by Brinkman's equation. The stream functions have been determined by matching the solutions. Some well known results are also deduced from the present study. The drag force experienced by capsule is calculated and its variation with respect to the fluid parameters is studied numerically and graphically as well.

2. MATHEMATICAL FORMULATION AND SOLUTION OF THE PROBLEM

We consider steady, axis-symmetric, creeping flow of a viscous and incompressible Newtonian fluid (region I) of viscosity μ_1 with a constant uniform velocity U at infinity relative to the spherical capsule with radius b comprises the drop of a Reiner-Rivlin liquid (region III) of viscosity μ_3 with radius a covered by a permeable layer (region II) with thickness δ, porosity ε, and permeability κ with the assumption that the fluid outside the capsule penetrates into the permeable layer but is not mingled with the liquid in the region III. The flow field due to the motion of the uniform stream of a steady, incompressible Newtonian fluid past the encapsulated drop of radius b is to be determined in the absence of body forces and couples. We take into consideration that the inner flow (region III) is also steady and incompressible. Further, we assume that the capsule to be stationary having its center at the origin of the spherical co-ordinates system (R, θ, ϕ) and taking $\theta = 0$ as an axis in the direction of the free stream flow directed along the + ve z-direction as depicted in Fig.1. The parameters pertaining to the exterior, the permeable layer, and the interior of the liquid capsule to be distinguished by the index in the superscripts under the bracket of an entity

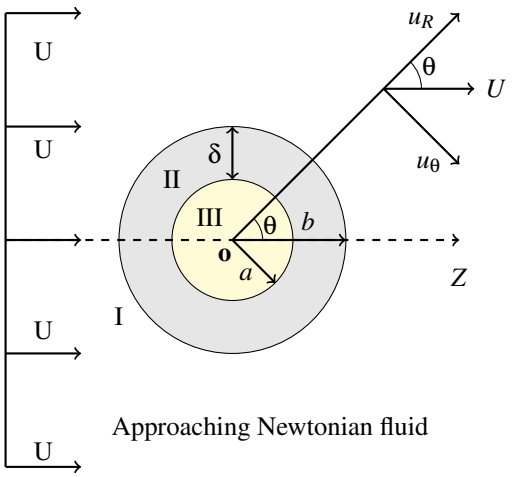

Fig. 1. Schematic representation of flow

$\chi^{(i)}$, $i = 1,2,3$ related to the region I ($i = 1$), region II ($i = 2$) and region III ($i = 3$) respectively.

Within the unimpeded fluid in the region I, outside the capsule, the Stokes and continuity equations characterize the prevailing flowfield as follows:

$$\mu_1 \tilde{\nabla}^2 \tilde{\mathbf{u}}^{(1)} = \tilde{\nabla} \tilde{p}^{(1)}, \quad b \le R < \infty \tag{1}$$

and

$$\tilde{\nabla} \cdot \tilde{\mathbf{u}}^{(1)} = 0, \quad b \le R < \infty \tag{2}$$

and the corresponding flowfield equations governing the motion of the fluid within the permeable region are described by the Brinkman and continuity equations with inertial terms omitted, respectively, as

$$\tilde{\nabla}^2 \tilde{\mathbf{u}}^{(2)} - \left(\frac{\alpha}{b}\right)^2 \tilde{\mathbf{u}}^{(2)} = \frac{1}{\mu_e} \tilde{\nabla} \tilde{p}^{(2)}, \quad a \le R \le b \tag{3}$$

and

$$\tilde{\nabla} \cdot \tilde{\mathbf{u}}^{(2)} = 0, \quad a \le R \le b, \tag{4}$$

$\alpha^2 = \frac{\mu_1 b^2}{\mu_e \kappa}$ is the dimensionless parameter pertaining to the permeable region, μ_1 is the viscosity of the clear fluid, μ_e is an effective viscosity of the permeable shell and κ is the permeability of the permeable shell. The velocity vector and the pressure for region I and II are, respectively, denoted by $\tilde{\mathbf{u}}^{(i)}$ and $\tilde{p}^{(i)}$, $i = 1,2$.

The constitutive equation for isotropic non-Newtonian Reiner-Rivlin liquid in the region III takes the form

$$\tilde{\tau}_{ij} = -\tilde{p}^{(3)} \delta_{ij} + 2\mu_3 \tilde{d}_{ij} + \mu_c \tilde{d}_{ik} \tilde{d}_{kj}, \tag{5}$$

where

$$\tilde{d}_{ij} = \frac{1}{2}(\tilde{u}^{(3)}_{i,j} + \tilde{u}^{(3)}_{j,i}),$$

$\tilde{\tau}_{ij}$ is the stress tensor, $\tilde{d}_{ij}$ is the rate of strain (deformation) tensor, $\tilde{p}^{(3)}$ is an arbitrary hydrostatic pressure, μ_3 is the coefficient of viscosity and μ_c is the coefficient of cross-viscosity of Reiner-Rivlin liquid in region III.

Taking in view of the axial symmetry flow in which all the flow functions are independent of ϕ, the velocity vector $\tilde{\mathbf{u}} = (\tilde{u}_R, \tilde{u}_\theta, 0)$ can be expressed by introducing the stream function through

$$\tilde{u}_R = \frac{-1}{R^2 \sin\theta} \frac{\partial \tilde{\psi}}{\partial \theta}, \quad \tilde{u}_\theta = \frac{1}{R \sin\theta} \frac{\partial \tilde{\psi}}{\partial r}. \tag{6}$$

In order to non-dimensionalize the quantities and operators appearing in the governing equations, we insert the following non-dimensional variables

$$R = br, \quad \tilde{u}_R = U u_r, \quad \tilde{u}_\theta = U u_\theta, \quad \tilde{\tau}_{ij} = \mu_i \frac{U}{b} \tau_{ij},$$
$$\tilde{d}_{ij} = \frac{U}{b} d_{ij}, \quad \tilde{p} = \mu_i \frac{U}{b} p, \quad \tilde{\psi} = U b^2 \psi,$$

where U and b represent some typical velocity and length of the flow field, respectively.

Introducing the stream function, we write for the internal flow within the liquid drop (region III) of radius a as follows

$$\psi^{(3)} = \psi_0 + \psi_1 S + \psi_2 S^2 + \ldots..,$$
$$p^{(3)} = p_0 + p_1 S + p_2 S^2 + \ldots....., \tag{7}$$

where S is the dimensionless number $\frac{\mu_c U}{\mu_3 b}$ assumed to be small. It can be shown by Ramkissoon (1989) that the Stokes approximation of momentum equation for Reiner-Rivlin fluid provides

$$E^4 \psi_0 = 0, \quad E^4 \psi_1 = 8r \sin^2\theta \cos\theta,$$
$$E^4 \psi_2 = \frac{32}{3} r^2 \sin^2\theta, \tag{8}$$

where

$$E^2 = \frac{\partial^2}{\partial r^2} + \frac{\sin\theta}{r^2} \frac{\partial}{\partial \theta} \left(\frac{1}{\sin\theta} \frac{\partial}{\partial \theta} \right). \tag{9}$$

Particular solutions of the equations (8) are given by

$$\psi_0 = (r^4 - r^2) \sin^2\theta, \quad \psi_1 = \frac{2}{21} r^5 \sin^2\theta \cos\theta,$$
$$\psi_2 = \frac{2}{63} r^6 \sin^2\theta. \tag{10}$$

Eliminating the pressures from the Eqs. (1) and (3), the stream function formulation of these equations for regions I and II get reduced, respectively, into the following non-dimensional forms

$$E^4 \psi^{(1)} = 0, \tag{11}$$

and

$$E^2(E^2-\alpha^2)\psi^{(2)}=0, \tag{12}$$

where the second order differential operator is given in Eq. (9).

The surviving velocity components are

$$u_r^{(i)}=\frac{-1}{r^2\sin\theta}\frac{\partial\psi^{(i)}}{\partial\theta}, \quad u_\theta^{(i)}=\frac{1}{r\sin\theta}\frac{\partial\psi^{(i)}}{\partial r}. \tag{13}$$

The dimensionless expression of tangential and normal stresses for region I and II, respectively, are given by

$$\tau_{r\theta}^{(i)}=\frac{1}{r\sin\theta}\left[\frac{\partial^2\psi^{(i)}}{\partial r^2}-\frac{2}{r}\frac{\partial\psi^{(i)}}{\partial r}\right]- -\frac{1}{r\sin\theta}\left[\frac{\sin\theta}{r^2}\frac{\partial}{\partial\theta}\left(\frac{1}{\sin\theta}\frac{\partial\psi^{(i)}}{\partial\theta}\right)\right], \tag{14}$$

$$\tau_{rr}^{(i)}=-p^{(i)}+\frac{2\mu_1}{r^2\sin\theta}\left[\frac{2}{r}\frac{\partial\psi^{(i)}}{\partial\theta}\right]+ +\frac{2\mu_1}{r^2\sin\theta}\left[\frac{\partial^2\psi^{(i)}}{\partial r\partial\theta}\right], \quad i=1,2. \tag{15}$$

Also, the dimensionless pressures in both the regions may be evaluated by integrating the following relations

$$\frac{\partial p^{(1)}}{\partial r}=-\frac{1}{r^2\sin\theta}\frac{\partial}{\partial\theta}(E^2\psi^{(1)}); \quad \frac{\partial p^{(1)}}{\partial\theta}=\frac{1}{r\sin\theta}\frac{\partial}{\partial r}(E^2\psi^{(1)}), \tag{16}$$

$$\frac{\partial p^{(2)}}{\partial r}=-\frac{\mu_e/\mu_1}{r^2\sin\theta}\frac{\partial}{\partial\theta}[(E^2-\alpha^2)\psi^{(2)}], \quad \frac{\partial p^{(2)}}{\partial\theta}=\frac{\mu_e/\mu_1}{r\sin\theta}\frac{\partial}{\partial r}[(E^2-\alpha^2)\psi^{(2)}]. \tag{17}$$

In case of axisymmetric incompressible creeping flow, the particular regular solutions of Stokes equation (11) by Happel and Brenner (1983), and Brinkman equation (12) by Zlatanovski (1999) on the symmetry axis in spherical polar coordinates, respectively, may be taken as

$$\psi^{(1)}(r,\zeta)=[A_2^\star r^{-1}+r^2+C_2^\star r]G_2(\zeta), 1\le r<\infty, \tag{18}$$

and

$$\psi^{(2)}(r,\zeta)=[A_2r^{-1}+B_2r^2+C_2y_{-2}(\alpha r)+ +D_2y_2(\alpha r)]G_2(\zeta), \quad l\le r\le 1 \tag{19}$$

where $l=a/b$, and $A_2^\star$, $C_2^\star$, A_2, B_2, C_2, D_2 are constants to be determined, $y_{-2}(\alpha r)=\alpha\sinh(\alpha r)-\frac{1}{r}\cosh(\alpha r)$, $y_2(\alpha r)=\alpha\cosh(\alpha r)-\frac{1}{r}\sinh(\alpha r)$, and $G_2(\zeta)$ is Gegenbauer function defined in Abramowitz and Stegun (1970).

While for flow within the Reiner-Rivlin drop in region III, we may take Ramkissoon (1989)

$$\psi^{(3)}=\psi_0+\psi_1S+\psi_2S^2+\sum_{n=2}^{\infty}[a_nr^n+b_nr^{n+2}]G_n(\zeta). \tag{20}$$

With the aid of the Eq.(10), we can now write the Eq. (20) explicitly in the form:

$$\psi^{(3)}(r,\zeta)=[(a_2-2)r^2+(b_2+2)r^4+\frac{4}{63}S^2 r^6]G_2(\zeta)+[a_3r^3+(b_3+\frac{4}{21}S)r^5]G_3(\zeta) +\sum_{n=4}^{\infty}[a_nr^n+b_nr^{n+2}]G_n(\zeta), \quad r\le l. \tag{21}$$

3. Boundary Conditions and Determination of Arbitrary Constants

The unknown appearing in Eqs. (18), (19) and (21) to be determined by the following boundary conditions:

On the outer shell surface $r=1$

(i). Continuity of velocity components implies that we may take

$$\psi^{(1)}=\psi^{(2)} \quad \text{and} \quad \frac{\partial\psi^{(1)}}{\partial r}=\frac{\partial\psi^{(2)}}{\partial r}. \tag{22}$$

(ii). Also, we assume that the tangential and normal components of stresses are continuous across the surface, so we can take

$$\tau_{r\theta}^{(1)}=\tau_{r\theta}^{(2)} \quad \text{and} \quad \tau_{rr}^{(1)}=\tau_{rr}^{(2)} \tag{23}$$

On the inner shell surface $r=l(a/b)$

(iii). Impenetrability at the inner shell surface requires that

$$\psi^{(2)}=0, \quad \psi^{(3)}=0. \tag{24}$$

(iv). Continuity of tangential velocity requires that

$$\frac{\partial\psi^{(2)}}{\partial r}=\frac{\partial\psi^{(3)}}{\partial r}. \tag{25}$$

(v). We further assume that the theory of interfacial tension is applicable to our problem. This means that the presence of interfacial tension only produces a discontinuity in the normal

stress τ_{rr} and does not in any way affect tangential stress $\tau_{r\theta}$. i.e. $\tau^{(2)}_{r\theta} = \tau^{(3)}_{r\theta}$ which can be shown to be equivalent to

$$\mu_1 \frac{\partial}{\partial r}\left(\frac{1}{r^2}\frac{\partial \psi^{(2)}}{\partial r}\right) = \mu_3 \frac{\partial}{\partial r}\left(\frac{1}{r^2}\frac{\partial \psi^{(3)}}{\partial r}\right). \quad (26)$$

As a result of the employment of boundary conditions (Eqs. (22)–(26)) , we are led to the following linear equations:

$$A_2^\star + C_2^\star - A_2 - B_2 - C_2 y_{-2}(\alpha) - D_2 y_2(\alpha) + 1 = 0, \quad (27)$$

$$-A_2^\star + C_2^\star + A_2 - 2B_2 - [\alpha^2 y_{-1}(\alpha) - y_{-2}(\alpha)]C_2 - [\alpha^2 y_1(\alpha) - y_2(\alpha)]D_2 + 2 = 0, \quad (28)$$

$$6A_2^\star - 6A_2 - [(\alpha^2+6)y_{-2}(\alpha) - 2\alpha^2 y_{-1}(\alpha)]C_2 - [(\alpha^2+6)y_2(\alpha) - 2\alpha^2 y_1(\alpha)]D_2 = 0, \quad (29)$$

$$6A_2^\star + 3C_2^\star - \left(\frac{\mu_e \alpha^2}{2\mu_1} + 6\right)A_2 + \frac{\mu_e \alpha^2}{\mu_1}B_2 + 2[-3y_{-2}(\alpha) + \alpha^2 y_{-1}(\alpha)]C_2 + 2[-3y_2(\alpha) + \alpha^2 y_1(\alpha)]D_2 = 0, \quad (30)$$

$$l^2 a_2 + l^4 b_2 - 2l^2 + 2l^4 + \frac{4}{63}S^2 l^6 = 0, \quad (31)$$

$$l^{-1}A_2 + l^2 B_2 + C_2 y_{-2}(\alpha l) + D_2 y_2(\alpha l) = 0, \quad (32)$$

$$-l^{-2}A_2 + 2lB_2 + [-l^{-1}y_{-2}(\alpha l) + \alpha^2 y_{-1}(\alpha l)]C_2 + [-l^{-1}y_2(\alpha l) + \alpha^2 y_1(\alpha l)]D_2 - 2la_2 - 4l^3 b_2 + 4l - 8l^3 - \frac{8}{21}S^2 l^5 = 0, \quad (33)$$

$$4\lambda^2 l^{-5}A_2 - 2\lambda^2 l^{-2}B_2 + \lambda^2[(l^{-2}\alpha^2 + 4l^{-4})y_{-2}(\alpha l) - 2\alpha^2 l^{-3}y_{-1}(\alpha l)]C_2 + \lambda^2[(l^{-2}\alpha^2 + +4l^{-4})y_2(\alpha l) - 2\alpha^2 l^{-3}y_1(\alpha l)]D_2 + 2l^{-2}a_2 - 4b_2 - 4l^{-2} - 8 - \frac{8}{7}S^2 l^2 = 0, \quad (34)$$

$$a_n l^n + b_n l^{n+1} = 0, \quad (35)$$

$$3a_3 l^2 + 5\left(b_3 + \frac{4}{21}S\right)l^4 = 0, \quad (36)$$

$$n a_n l^{n-1} + (n+2)b_n l^{n+1} = 0, \quad (37)$$

$$10\left(b_3 + \frac{4}{21}S\right)l = 0, \quad (38)$$

$$n(n-3)l^{n-4}a_n + (n-1)(n+2)l^{n-2}b_n = 0, \quad n \geq 4. \quad (39)$$

Solving the above system of linear Eqs. (27) to (39), we have determined all the unknowns appearing in the stream functions (18), (19) and (21) which are given in the appendix A.

Hence, the dimensionless stream functions for the flow fields corresponding to the regions I, II and III are now known, and they are given, respectively, as

$$\psi^{(1)}(r,\zeta) = [A_2^\star r^{-1} + r^2 + C_2^\star r]G_2(\zeta), 1 \leq r < \infty, \quad (40)$$

$$\psi^{(2)}(r,\zeta) = [A_2 r^{-1} + B_2 r^2 + C_2 y_{-2}(\alpha r) + + D_2 y_2(\alpha r)]G_2(\zeta), \qquad l \leq r \leq 1 \quad (41)$$

and

$$\psi^{(3)}(r,\zeta) = [(a_2 - 2)r^2 + (b_2+2)r^4 + + \frac{4}{63}S^2 r^6]G_2(\zeta), \qquad r \leq l \quad (42)$$

where the values of arbitrary constants $A_2^\star$, $C_2^\star$, A_2, B_2, C_2, D_2, a_2, and b_2 are listed in the appendix A.

4. Evaluation of Drag on Capsule

The drag force F to the capsule by external fluid is evaluated by integrating the normal and tangential stresses over the surface by Happel and Brenner (1965) as follows

$$F = 2\pi b^2 \int_0^\pi \left(\tau^{(1)}_{rr}\cos\theta - \tau^{(1)}_{r\theta}\sin\theta\right)_{r=1} \sin\theta d\theta. \quad (43)$$

On evaluating dimensional stress-components, we get

$$\tau^{(1)}_{rr} = \frac{U\mu_1}{b}\left(\frac{3C_2^\star}{r^2} + \frac{6A_2^\star}{r^4}\right)\cos\theta,$$

and

$$\tau^{(1)}_{r\theta} = \frac{3U\mu_1 A_2^\star}{br^4}\sin\theta.$$

Substituting the values of $\tau^{(1)}_{rr}$ and $\tau^{(1)}_{r\theta}$ in Eq. (43) and integrating w.r.t. 'θ', we obtain

$$F = 2\pi b U\mu_1 \left\{\frac{2}{3}\left(\frac{3C_2^\star}{r^2} + \frac{6A_2^\star}{r^4}\right) - \frac{4A_2^\star}{r^4}\right\}, = 4\pi b U\mu_1 C_2^\star, \quad \text{at} \quad r = 1. \quad (44)$$

The ultimate expression for F is obtained by substituting for $C_2^\star$, and is presented in by Eq. (A.2) of the appendix A. The algebraic calculation leading to Eq. (A.2) is although unsophisticated but extremely cumbersome. However, the genuineness of $C_2^\star$ may be examined by considering few limiting cases for which the analytical solutions already exist in the literature.

5. RESULTS AND DISCUSSION

At the outset, it is instructive to consider some limiting situations of the drag force as discussed below:

As $a \to b$ (for a liquid sphere of radius b):

In this case, encapsulated drop reduces into the liquid sphere of radius b, and drag in this case comes out as

$$F = -\frac{2b\pi U\mu_1}{3(1+\lambda^2)}\left[6\lambda^2+9+\frac{32}{63}S^2\right]. \qquad (45)$$

Where $\lambda^2 = \mu_1/\mu_3$. This result was previously obtained by Ramkissoon (1989).

As $a \to 0$ (for a homogeneous permeable sphere of radius b):

The drag on the permeable sphere of radius b is obtained by letting the inner radius a to zero as follows

$$F = -\frac{12b\pi U\alpha^2\left[1-\frac{\tanh\alpha}{\alpha}\right]\mu_1}{3\alpha^2+3\left[1-\frac{\tanh\alpha}{\alpha}\right]}, \qquad (46)$$

this result agrees with a well-known result earlier reported by Brinkman (1947), Ooms *et al.* (1970), Neale *et al.* (1973), Masliyah *et al.* (1987), Qin and Kaloni (1988), Qin and Kaloni (1993), Vasin and Kharitonova (2011a), Vasin and Kharitonova (2011b) and later Yadav and Deo (2012) for the drag force experienced by a permeable sphere in an unbounded clear fluid.

As $\mu_3 \to \infty, S = 0$ (permeable sphere with solid core):

In this case, the drag on the permeable sphere with solid core is obtained as

$$\begin{aligned} F = &-2b\pi U\mu_1[567(2+l^3)\alpha^3\cosh(\delta\alpha)+3(-378\alpha^2 \\ &-189l^3\alpha^2+567l^2(-1+\alpha^2))\sinh(\delta\alpha)]/[189 \\ &\times(\alpha(3+3l^2+2\alpha^2+l^3\alpha^2)\cosh(\delta\alpha) \\ &-3(2l\alpha+(1-l^2\alpha^2)\sinh(\delta\alpha)))] \end{aligned} \qquad (47)$$

here $\delta = 1-l$. This is the same result Earlier reported byMasliyah *et al.* (1987).

As $\kappa \to 0$, when $l \to 1(\delta = 0)$ and $\mu_3 \to \infty$ (Stokes' force on a sphere of radius b):

$$F = -6b\pi U\mu_1, \qquad (48)$$

this is the well known Stokes force on a solid sphere as required.

NON-DIMENSIONAL DRAG

Dimensionless force D_N is defined as the ratio of the force F to the Stokes force $F_{st} = -6b\pi U\mu_1$ as follows

$$\begin{aligned} D_N &= \frac{F}{-6b\pi U\mu_1} \\ &= \frac{2}{3}C_2^\star, \end{aligned} \qquad (49)$$

here $C_2^\star$ is given in Eq. (A.2).The expression (49) therefore gives the drag force in non-dimensional form experienced by a capsule when a Newtonian fluid stream past it.

The drag coefficient D_N is plotted for numerous values of thickness of permeable layer(δ), ratio of viscosities (λ^2), dimensionless parameter S characterizing the cross viscosity of the Reiner-Rivlin liquid and permeability parameter (α) and its variation is depicted in Figs.2–7. Dependence of force D_N

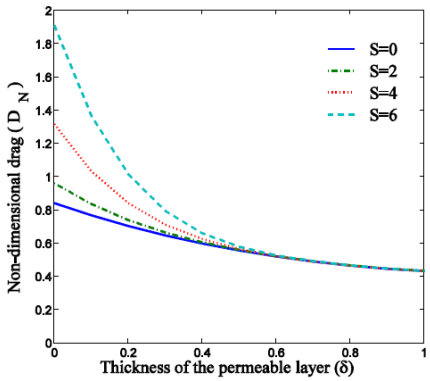

Fig. 2. Variations in dimensionless force D_N with respect to the parameter δ at $\lambda^2 = 1.5, \alpha = 2$ for various values of S.

on the dimensionless thickness of permeable layer δ at the various values of parameter S are shown in Fig.2. It is evident from the figure that the non-dimensional drag D_N decreases with increasing values of δ between 0 and 1 and increases with the increasing values of S. At $\delta = 0$, we deal with the liquid drop, and the drag on liquid drop is different for different values of S. It is obvious from the Fig.2 that the drag on Newtonian liquid drop ($S = 0$) is less than the drag on non-Newtonian liquid drop($S \neq 0$). It is also clear that for small values of $S(< 4)$ the decrements in D_N is slow and for higher values of $S(\geq 4)$ drag decreases rapidly. At $\delta \to 1$, the encapsulated drop becomes absolutely permeable and drag in this case becomes almost same and constant for all the values of S.

The variation of D_N with λ^2 is depicted in Fig.3 for various values of α which shows that corresponding to very low permeability parameter, drag decreases vary rapidly and as the permeability parameter increases, there takes place a slight decrease in drag and then it becomes almost constant with increasing λ^2. It is interesting to note that when the perme-

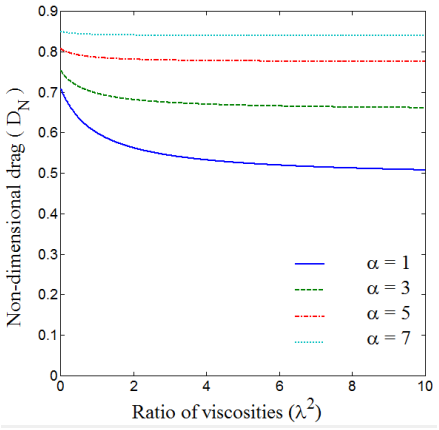

Fig. 3. Variations in drag coefficient D_N versus viscosity ratio λ^2 at $S = 0.5, \delta = 0.3$ for various values of permeability parameter α.

ability parameter α is very high, i.e. permeability is very low, the drag throughout is almost constant.

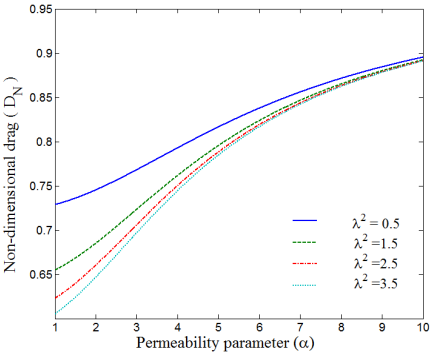

Fig. 4. Variations in drag coefficient D_N versus permeability parameter α at $S = 1, \delta = 0.2$ for various values of viscosity ratio λ^2.

The variation of the drag coefficient D_N with respect to permeability parameter α for various values of viscosity ratio λ^2 is shown in Fig.4. It can be observed from the Fig.4 that the drag D_N increases with increasing permeability parameterα , i.e., it decreases with permeability, for various values of relative viscosity λ^2 and initially increases very rapidly and then decreases very slowly with increasing viscosity ratio λ^2. Figures 5–7 depict the variation in non-dimensional drag with regard to S for $\lambda^2 = 0.2, 0.5, 0.7$ respectively. Figure 5 shows that the value of non-dimensional drag D_N on the permeable sphere increases with the increase of permeability parameter α for $S < 4.25$, and then it becomes almost constant for all the values of permeability parameter α, when $4.15 \leq S < 4.35$; but the value of D_N increases with decrease of permeability parameter α, when $S \geq 4.35$.

Figure 6 shows that the value of D_N on the permeable sphere increases as the dimensionless parameter S increases and increasing permeability parameter α as well, and it becomes almost constant for all values of permeability parameter α as $S \to 5$ for viscosity ratio $\lambda^2 = 1$. Whereas Fig.7 exhibits that the value of D_N on the permeable sphere increases differently for increasing permeability parameter α for $\lambda^2 = 1.5$ at $\delta = 0.2$. This variation of the drag coefficient D_N with S for the specified values of relative viscosity λ^2 can also be viewed in tables 1–3.

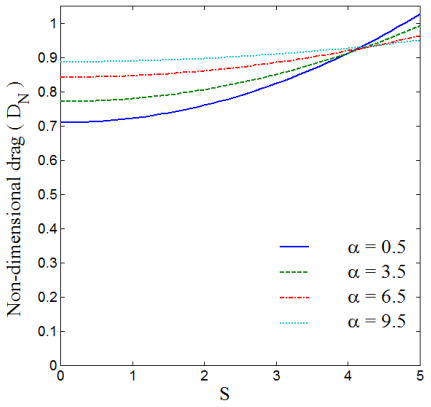

Fig. 5. The variation of non-dimensional drag D_N versus S for $\lambda^2 = 0.5$ at $\delta = 0.2$.

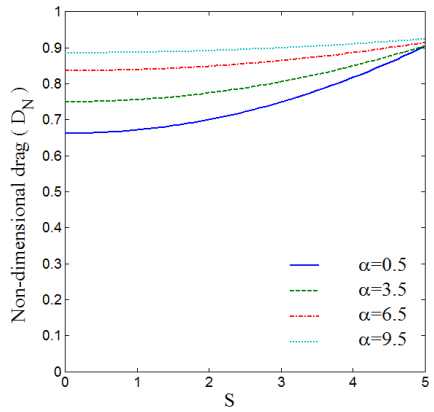

Fig. 6. The variation of non-dimensional drag D_N versus S for $\lambda^2 = 1.0$ at $\delta = 0.2$.

Table 1 Numerical values of D_N with respect to parameter S for various values of permeability parameter $\alpha; \delta = 0.2, \lambda^2 = 0.5$

S	Drag coefficient →			
↓	$\alpha = 0.5$	$\alpha = 3.5$	$\alpha = 6.5$	$\alpha = 9.5$
0	0.7100	0.7715	0.8422	0.8874
1	0.7227	0.7803	0.8471	0.8899
2	0.7608	0.8070	0.8617	0.8976
3	0.8243	0.8514	0.9103	0.9103
4	0.9132	0.9135	0.9202	0.9282
5	1.0274	0.9934	0.9640	0.9511

The numerical values of non-dimensional drag D_N for $\lambda^2 = 0.5$, $\lambda^2 = 1.0$, and $\lambda^2 = 1.5$ are presented, respectively, in Tables 1, 2 and 3, and the cor-

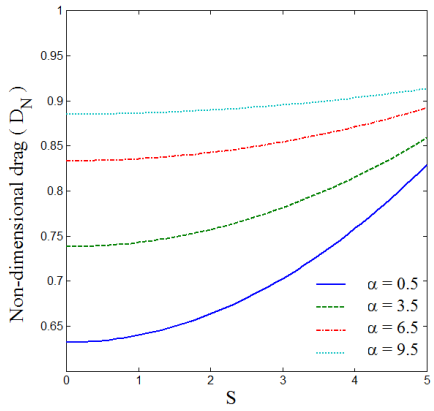

Fig. 7. The variation of non-dimensional drag D_N versus S for $\lambda^2 = 1.5$ at $\delta = 0.2$.

responding variations are shown in Figs.5–7. It may be seen from the tables that for the relative viscosity($\lambda^2 < 1$), the numerical values of the drag, for $S > 4$, decreases as permeability parameter increases which is in good agreement with the graphical representation of the drag, which may also be further checked experimentally. These values are useful in estimating of optimum drag profiles in low Reynolds number flows also.

Table 2 Numerical values of D_N with respect to parameter S for various values of permeability parameter $\alpha; \delta = 0.2, \lambda^2 = 1.0$

S	Drag coefficient →			
↓	$\alpha = 0.5$	$\alpha = 3.5$	$\alpha = 6.5$	$\alpha = 9.5$
0	0.6618	0.7498	0.8362	0.8858
1	0.6716	0.7560	0.8394	0.8874
2	0.7008	0.7748	0.8489	0.8922
3	0.7494	0.8062	0.8648	0.9000
4	0.8176	0.8500	0.8871	0.9111
5	0.9052	0.9064	0.9157	0.9253

Table 3 Numerical values of D_N with respect to parameter S for various values of permeability parameter $\alpha; \delta = 0.2, \lambda^2 = 1.5$

S	Drag coefficient →			
↓	$\alpha = 0.5$	$\alpha = 3.5$	$\alpha = 6.5$	$\alpha = 9.5$
0	0.6319	0.7498	0.8362	0.8851
1	0.6398	0.7560	0.8394	0.8863
2	0.6635	0.7748	0.8489	0.8897
3	0.7029	0.8062	0.8648	0.8954
4	0.7582	0.8500	0.8871	0.9034
5	8292	0.9064	0.9157	0.9137

6. CONCLUSION

The expressions for stream function solutions to the flow field equations for the steady axisymmetric Stokes flow of Newtonian fluid around the encapsulated drop of Reiner-Rivlin liquid are obtained. Various useful results are obtained from the solution, particularly the closed form expression for the drag force and the dependence of the dimensionless drag on the various fluid parameters. It has been found that an increase in the thickness of the permeable layer δ decreases the drag force experienced by the encapsulated drop. It is also observed that hydrodynamic drag, in general, is increasing or decreasing function of the permeability parameter α when the relative viscosity $\lambda^2 < 1$.The effect of the dimensionless parameter S on the drag for fixed values of the remaining fluid parameters is also studied and found that it increases the drag on the encapsulated drop.

REFERENCES

Abramowitz, M. and I. Stegun (1970). *Handbook of Mathematical Functions*. New York: Dover Publications.

Barman, B. (1996). Flow of a Newtonian fluid past an impervious sphere embedded in a porous medium. *Indian J. Pure Appl. Math. 27*(12), 1244–1256.

Bhatt, B. and N. Sacheti (1994). Flow past a porous spherical shell using the Brinkman model. *J. Phys D, Appl. Phys. 27*(1), 37–41.

Birikh, R. and R. Rudakoh (1982). Slow motion of a permeable sphere in a viscous fluid. *Fluid Dynamics 17*(5), 792–793.

Boutros, Y., M. A. el Malek, N. Badran, and H. Hassan (2006). Lie-group method of solution for steady two dimensional boundary layer stagnation point flow towards a heated stretching sheet placed in a porous medium. *Meccanica 41*(6), 681–691.

Brinkman, H. (1947). A calculation of viscous force exerted by a flowing fluid on dense swarm of particles. *Appl. Sci. Res.A1 1*(1), 27–34.

Darcy, H. (1856). *Les Fontaines Publiques De La Ville De Dijon*. Paris: Victor Dalmont.

Deo, S. and B. Gupta (2009). Stokes flow past a swarm of porous approximately spheroidal par-ticles with Kuwabara boundary condition. *Acta Mecheanica 203*(3-4), 241–254.

Deo, S. and B. Gupta (2010). Drag on a porous sphere embedded in another porous medium. *Journal of Porous Media 13*(11), 1009–1016.

Happel, J. and H. Brenner (1965). *Low Reynolds Number Hydrodynamics*. Englewood Cliffs, NJ: Prentice-Hall.

Happel, J. and H. Brenner (1983). *Low Reynolds Number Hydrodynamics*. Hague: Martinus Nijhoff, Publishers.

Higdon, J. and M. Kojima (1981). On the calculation of Stokes flow past porous particles. *Int. J. Multiphase Flow 7*(6), 719–727.

Jaiswal, B. and B. Gupta (2014a). Drag on Reiner-Rivlin liquid sphere placed in a micro- polar fluid with non-zero boundary condition for microrotations. *Int. J. of Appl. Math. and Mech. 10*(7), 90–103.

Jaiswal, B. and B. Gupta (2014b). Wall effects on Reiner-Rivlin liquid spheroid. *Appl. Compt. Mech. 8*(2), 157–176.

Jaiswal, B. and B. Gupta (2015). Brinkman flow of a viscous fluid past a Reiner-Rivlin liquid sphere immersed in a saturated porous medium. *Transport in Porous Media 106*(3), DOI: 10.1007/s11242–015–0472–2.

Joseph, D. and L. Tao (1964). The effect of permeability on the slow motion of a porous sphere in a viscous liquid. *Journal Appl. Math. Mech. 44*(8-9), 361–364.

Lundgren, T. (1972). Slow flow through stationary random beds and suspensions of spheres. *Journal of Fluid Mechanics 51*(2), 273–299.

Masliyah, J., G. Neale, K. Malysa, and T. V. de Ven (1987). Creeping flow over a composite sphere: Solid core with porous shell. *Chemical Engineering Science 4*(2), 245–253.

Masliyah, J. and M. Polikar (1980). Terminal velocity of porous spheres. *Canadian Journal of Chemical Engineering 58*(3), 299–302.

Matsumoto, K. and A. Suganuma (1977). Settling velocity of a permeable model floc. *Chemical Engineering Science 32*(4), 445–447.

Mukhopadhyay, S. and G. Layek (2009). Radiation effect on forced convective flow and heat transfer over a porous plate in a porous medium. *Meccanica 44*(5), 587–597.

Nandkumar, K. and J. Masliyah (1982). Laminar flow past a permeable sphere. *Canadian Journal of Chemical Engineering 60*(2), 202–211.

Neale, G., N. Epstein, and W. Nader (1973). Creeping flow relative to permeable spheres. *Chemical Engineering Science 28*(10), 1865–1873.

Ooms, G., P. Mijulieff, and H. Becker (1970). Frictional force exerted by a flowing fluid in a permeable particle with particular reference to polymer coils. *Journal of Chemical Physics 53*(11), 4123–4130.

Padmavathi, B., T. Amarnath, and D. Palaniappan (1994). Stokes flow about a porous spherical particle. *Archives of Mechanics 46*(3), 191–199.

Prakash, J., G. P. R. Sekhar, and M. Kohr (2011). Stokes flow of an assemblage of porous particles: Stress jump condition. *journal Appl. Math. Phys. 62*(6), 1027–1046.

Qin, Y. and P. Kaloni (1988). A Cartesian-tensor solution of Brinkman equation. *Journal of Engineering Mathematics 22*(2), 177–188.

Qin, Y. and P. Kaloni (1993). Creeping flow past a spherical shell. *Journal of Applied Mathematics and Mechanics 73*(2), 77–84.

Ramkissoon, H. (1989). Stokes flow past a Reiner-Rivlin fluid sphere. *Journal of Applied Mathematics and Mechanics 69*(8), 259–261.

Ramkissoon, H. and K. Rahaman (2001). Non-Newtonian fluid sphere in a spherical container. *Acta Mechanica 149*(1-4), 239–245.

Sekhar, G. P. R. and A. Bhattacharyya (2005). Stokes flow inside a porous spherical shell: Stress jump boundary condition. *journal Appl. Math. Phys. 56*(3), 475–496.

Srinivasacharya, D. (2003). Creeping flow past a porous approximate sphere. *Journal of Applied Math. Mech. 83*(7), 499–504.

Srinivasacharya, D. (2005). Motion of a porous sphere in a spherical container. *Mecanique 333*(8), 612–616.

Sutherland, D. and C. Tan (1970). Sedimentation of a porous sphere. *Chemical Engineering Science 25*(12), 1948–1950.

Tam, C. (1969). The drag on a cloud of spherical particles in a low Reynolds number flow. *Journal of Fluid Mechanics 38*(3), 537–546.

Vasin, S. and T. Kharitonova (2011a). Uniform liquid flow around porous spherical shell. *Colloid Journal 73*(1), 18–23.

Vasin, S. and T. Kharitonova (2011b). Uniform liquid flow around porous spherical shell. *Colloid Journal 73*(3), 297–302.

Yadav, P. and S. Deo (2012). Stokes flow past a porous spheroid embedded in another porous medium. *Meccanica 47*(6), 1499–1516.

Yadav, P., A. Tiwari, S. Deo, A. Filippov, and S. Vasin (2010). Hydrodynamic permeability of membranes built up by spherical particles covered by porous shells: Effect of stress jump condition. *Acta Mechanica 215*(1-4), 193–209.

Zlatanovski, T. (1999). Axisymmetric creeping flow past a porous prolate spheroidal particle using the Brinkman model. *Q. J. Mech. Appl. Math. 52*(1), 111–126.

APPENDIX A:

Determination of arbitrary constants

Solving the Eqs. (27) to (39) for the special case $\mu_e = \mu_1$, we obtain the surviving coefficients as given below

$$(A.1)\quad A_2^\star = -\left(-2l(16l^7S^2\alpha^2+32l^4S^2(3+\alpha^2)-189(3+2\lambda^2))+3\alpha(64l^6S^2+84l\alpha^2\lambda^2+42l^4\alpha^2\lambda^2 + 126l^2(3+2\lambda^2)-21l^3\alpha^2(3+2\lambda^2)-42(6+\alpha^2)(3+2\lambda^2))\cosh(\delta\alpha)+3(32l^6S^2(1+ +\alpha^2)-21l^4\alpha^2(-3+\alpha^2)\lambda^2-42l(-6+3\alpha^2+\alpha^4)\lambda^2+63l^3\alpha^2(3++2\lambda^2)-63l^2(-3+ +\alpha^2)(3++2\lambda^2)+126(2+\alpha^2)(3+2\lambda^2))\sinh(\delta\alpha))/(126\Delta),$$

$$(A.2)\quad C_2^\star = -\left(32l^5(2+l^3)S^2\alpha^3+189(2+l^3)\alpha^3(3+2\lambda^2)\cosh(\delta)+\alpha 3(32l^6S^2(-1+\alpha^2)+126l\alpha^2 \times(-1+\alpha^2)\lambda^2+63l^4\alpha^2(-1+\alpha^2)\lambda^2-126\alpha^2(3+2\lambda^2)-63l^3\alpha^2(3+2\lambda^2)+189l^2(-1 +\alpha^2)(3+2\lambda^2))\sinh(\delta\alpha))/(126\Delta),$$

$$(A.3)\quad A_2 = -\left(l(2\alpha^3(567+16l^7S^2+378\lambda^2)+l^2\alpha^3(567+64l^3S^2+378\lambda^2)\cosh(\delta\alpha)+l(32l^4S^2(-3 +3\alpha^2+2\alpha^4)+189l^2\alpha^2(-1+\alpha^2)\lambda^2-189l\alpha^2(3+2\lambda^2)-567(1-\alpha^2)(3+2\lambda^2)) \times\sinh(\delta\alpha)))/(63\alpha^2\Delta),$$

$$(A.4)\quad B_2 = -\left(l\alpha(567-32l^4S^2+378\lambda^2)+\alpha(32l^6S^2-189(3+2\lambda^2))\cosh(\delta\alpha)+(32l^6S^2\alpha^2-189l \times(-1+\alpha^2)\lambda^2+189(3+2\lambda^2))\sinh(\delta\alpha))/(63\Delta),$$

$$(A.5)\quad C_2 = -\left(l\alpha(32l^7S^2\alpha^2+32l^4S^2(3+2\alpha^2)+567(3+2\lambda^2))\cosh(\alpha)-3(l\alpha(32l^5S^2+126\alpha^2\lambda^2+ +63l^3\alpha^2\lambda^2+189l(3+2\lambda^2))\cosh(l\alpha)+l(567+32l^4S^2+378\lambda^2)\sinh(\alpha)-(32l^6S^2+ +126l\alpha^2\lambda^2+63l^4\alpha^2\lambda^2+189l^2(3+2\lambda^2)+126\alpha^2(3+2\lambda^2)+63l^3\alpha^2(3+2\lambda^2)) \times\sinh(l\alpha)))/(63\alpha^2\Delta),$$

$$(A.6)\quad D_2 = +\left(-3l(567+32l^4S^2+378\lambda^2)\cosh(\alpha)+3(32l^6S^2+126l\alpha^2\lambda^2+63l^4\alpha^2\lambda^2+189l^2(3+ +2\lambda^2)+126\alpha^2(3+2\lambda^2)+63l^3\alpha^2(3+2\lambda^2))\cosh(\delta\alpha)+l\alpha((32l^7S^2\alpha^2+32l^4S^2(3+ +2\alpha^2)+567(3+2\lambda^2))\sinh(\alpha)-3(32l^5S^2+126\alpha^2\lambda^2+63l^3\alpha^2\lambda^2+189l(3+2\lambda^2)) \times\sinh(l\alpha)))/(63\alpha^2\Delta),$$

$$(A.7)\quad a_2 = -\left(3\alpha(126\alpha^2\lambda^2+63l^3\alpha^2\lambda^2+504l(3+2\lambda^2)+16l^5S^2(7+2\lambda^2))-4\alpha(126l\alpha^2\lambda^2+4l^5S^2 \times\alpha^2\lambda^2+2l^8S^2\alpha^2\lambda^2++189l^2(3+2\lambda^2)+63l^3\alpha^2(3+2\lambda^2)+63(3+2\alpha^2)(3++2\lambda^2)+ +6l^6S^2(7+2\lambda^2)+2l^7S^2\alpha^2(7+2\lambda^2)+l^4(63\alpha^2\lambda^2+2S^2(3+2\alpha^2)(7+2\lambda^2)))\cosh(\delta\alpha)- -(8l^8S^2\alpha^4\lambda^2+8l^5S^2(-3+3\alpha^2+2\alpha^4)\lambda^2+63l(-3+3\alpha^2+8\alpha^4)\lambda^2-756(3+2\lambda^2)+ +756l^2\alpha^2(3+2\lambda^2)+24l^6S^2\alpha^2(7+2\lambda^2)-12l^4(-21\alpha^{42}+2S^2(7+2\lambda^2))) \times\sinh(\delta\alpha))/(126\Delta),$$

$$(A.8)\quad b_2 = -\left(-3\alpha(126\alpha^2\lambda^2+32l^5S^2(5+2\lambda^2)+63l^3(24+(16+\alpha^2)\lambda^2))+4l^2\alpha(126l\alpha^2\lambda^2+4l^6S^2 \times\alpha^2\lambda^2+63(3+2\alpha^2)(3+2\lambda^2)+4l^5S^2\alpha^2(5+2\lambda^2)+l^3\alpha^2(189+2(63+4S^2)\lambda^2)+3l^4 \times(21\alpha^2\lambda^2+4S^2(5+2\lambda^2))+l^2(189(3+2\lambda^2)+4S^2(3+2\alpha^2)(5+2\lambda^2)))\cosh(\delta\alpha)+ +l(16l^7S^2\alpha^4\lambda^2-567(-1+\alpha^2)\lambda^2+252l^2(-3+3\alpha^2+2\alpha^4)\lambda^2++16l^4S^2(-3+3\alpha^2+ +2\alpha^4)\lambda^2-756l(3+2\lambda^2)+12l^5\alpha^2(21\alpha^2\lambda^2+4S^2(5+2\lambda^2))-12l^3(-63\alpha^2(3+2\lambda^2)+ +4S^2(5+2\lambda^2)))\sinh(\delta\alpha))/(126l^2\Delta),$$

where

$$\Delta = -6l\alpha(3+2\lambda^2)+\alpha(2l\alpha^2\lambda^2+l^4\alpha^2\lambda^2+l^3\alpha^2(3+2\lambda^2)+(3+2\alpha^2)(3+2\lambda^2)+l^2(9+6\lambda^2))$$
$$\times\cosh(\delta\alpha)+(-9-6\lambda^2+l^4\alpha^4\lambda^2+l(-3+3\alpha^2+2\alpha^4)\lambda^2+3l^2\alpha^2(3+2\lambda^2))\sinh(\delta\alpha),$$
$$\alpha=\frac{b}{\sqrt{\kappa}},\quad \delta=1-l,\quad \lambda^2=\frac{\mu_1}{\mu_3}.$$

APPENDIX B:

The Gegenbauer functions $G_n(\zeta)$ of first kind are the solutions of the following differential equation, which are the polynomials of degree n

$$(1-\zeta^2)\frac{d^2\psi}{d\zeta^2}+n(n-1)\psi=0, \tag{B.1}$$

where the Gegenbauer polynomials $G_n(\zeta)$ are related to the Legendre polynomials of degree n by the following relation

$$G_n(\zeta)=\frac{P_{n-1}(\zeta)-P_n(\zeta)}{2n-1},\quad n\geq 2. \tag{B.2}$$

The governing equation in the stream function solution of Brinkman equation takes the following form

$$r^2\frac{d^2R}{dr^2}+[\alpha^2r^2+n(n-1)]R=0. \tag{B.3}$$

The linearly independent solutions of (B.3) are $\sqrt{\alpha r}I_\nu(\alpha r)$ and $\sqrt{\alpha r}I_{-\nu}(\alpha r)$.

To facilitate our calculation, we have utilized the under-mentioned notations in dimensionless form

$$y_n(\alpha r)=\sqrt{\frac{\pi\alpha r}{2}}\alpha^\nu I_\nu(\alpha r)\quad\text{and}\quad y_{-n}(\alpha r)=\sqrt{\frac{\pi\alpha r}{2}}\alpha^\nu I_{-\nu}(\alpha r),\quad \nu=\frac{n-1}{2}. \tag{B.4}$$

In particular,

$$y_1(\alpha r)=\sinh(\alpha r);\qquad y_{-1}(\alpha r)=\cosh(\alpha r), \tag{B.5}$$
$$y_2(\alpha r)=\alpha\cosh(\alpha r)-\frac{1}{r}\sinh(\alpha r);\qquad y_{-2}(\alpha r)=\alpha\sinh(\alpha r)-\frac{1}{r}\cosh(\alpha r).$$